

# SINGLE-ATOM TRANSISTORS: ATOMIC-SCALE ELECTRONIC DEVICES IN EXPERIMENT AND SIMULATION

FANG-QING XIE<sup>1,4</sup>, ROBERT MAUL<sup>2,3,4</sup>,  
WOLFGANG WENZEL<sup>4,5</sup>, GERD SCHÖN<sup>3,4,5</sup>,  
CHRISTIAN OBERMAIR<sup>1,4</sup> AND THOMAS SCHIMMEL<sup>1,4,5,\*</sup>

<sup>1</sup>Institute of Applied Physics, Karlsruhe Institute of Technology (KIT),  
Campus South, 76131 Karlsruhe, Germany

<sup>2</sup>Steinbuch Centre of Computing, Karlsruhe Institute of Technology,  
Campus North, 76021 Karlsruhe, Germany

<sup>3</sup>Institut für Theoretische Festkörperphysik, Karlsruhe Institute of Technology (KIT),  
Campus South, 76131 Karlsruhe, Germany

<sup>4</sup>Center for Functional Nanostructures (CFN), Karlsruhe Institute of Technology  
(KIT), 76131 Karlsruhe, Germany

<sup>5</sup>Institute of Nanotechnology, Forschungszentrum Karlsruhe, Karlsruhe Institute of  
Technology (KIT), 76021 Karlsruhe, Germany

**E-MAIL:** \*[thomas.schimmel@physik.uni-karlsruhe.de](mailto:thomas.schimmel@physik.uni-karlsruhe.de)

*Received: 1<sup>st</sup> September 2010 / Published: 13<sup>th</sup> June 2011*

## ABSTRACT

Controlling the electronic conductivity on the quantum level will impact the development of future nanoscale electronic circuits with ultra-low energy consumption. Here we report about the invention of the single-atom transistor, a device which allows one to open and close an electronic circuit by the controlled and reproducible repositioning of one single atom. The atomic switching process is induced by a voltage applied to an independent, third “gate” electrode. In addition to the demonstration of *single*-atom switches, the controlled and reproducible operation of *multi*-atom quantum switches is demonstrated both in experiment and in atomistic calculation. Atomistic modelling of structural and conductance properties elucidates bistable electrode

reconstruction as the underlying operation mechanism of the devices. Atomic transistors open intriguing perspectives for the emerging fields of quantum electronics and logics on the atomic scale.

## INTRODUCTION

Fascinating physical properties and technological perspectives have motivated investigation of atomic-scale metallic point contacts in recent years [1 – 10]. The quantum nature of the electron is directly observable in a size range where the width of the contacts is comparable to the Fermi wavelength of the electrons, and conductance is quantized in multiples of  $2e^2/h$  for ballistic transport through ideal junctions [2].

In metallic point contacts, which have been fabricated by mechanically controlled deformation of thin metallic wires [2–4] and electrochemical fabrication techniques [1, 5–7] the conductance depends on the chemical valence [2, 3]. Two-terminal conductance-switching devices based on quantum point contacts were developed both with an STM-like setup [8] and with electrochemical methods [9].

In our new approach, a three-terminal, gate-controlled atomic quantum switch was fabricated by electrochemical deposition of silver between two nanoscale gold electrodes (see Fig. 1) [1, 6]. A comparison of the experimental data with theoretical calculations indicates perfect atomic order within the contact area without volume or surface defects [10].

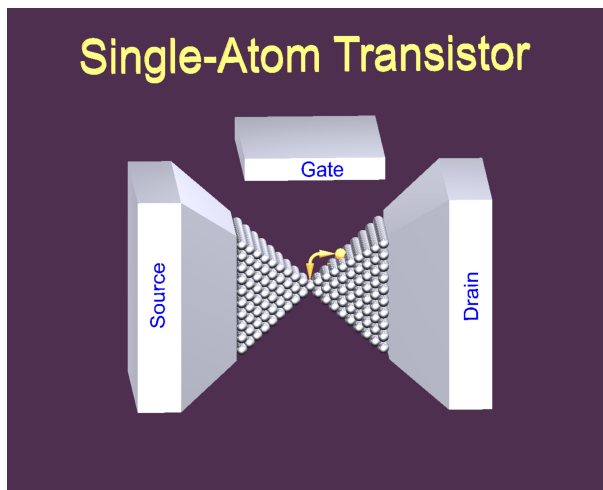


**Figure 1.** Schematic of the single-atom transistor: The atomic switch is entirely controlled by an independent third gate electrode, allowing to open and close a metallic contact between the source and drain electrodes by the gate-voltage controlled relocation of one single silver atom.

---

## SWITCHING AN ATOM

We control individual atoms in the quantum point contact by a voltage applied to an independent gate electrode, which allows a reproducible switching of the contact between a quantized conducting “on-state” and an insulating “off-state” without any mechanical movement of an electrode (see Fig. 2).

To fabricate the initial atomic-scale contact we deposit silver within a narrow gap between two macroscopic gold electrodes (gap width: typically 50 nm) by applying an electrochemical potential of 10–40 mV to a gate electrode [7]. The gold electrodes are covered with an insulating polymer coating except for the immediate contact area, and serve as electrochemical working electrodes. They correspond to the “source” and “drain” electrodes of the atomic-scale transistor. Two silver wires serve as counter and quasi-reference electrodes.

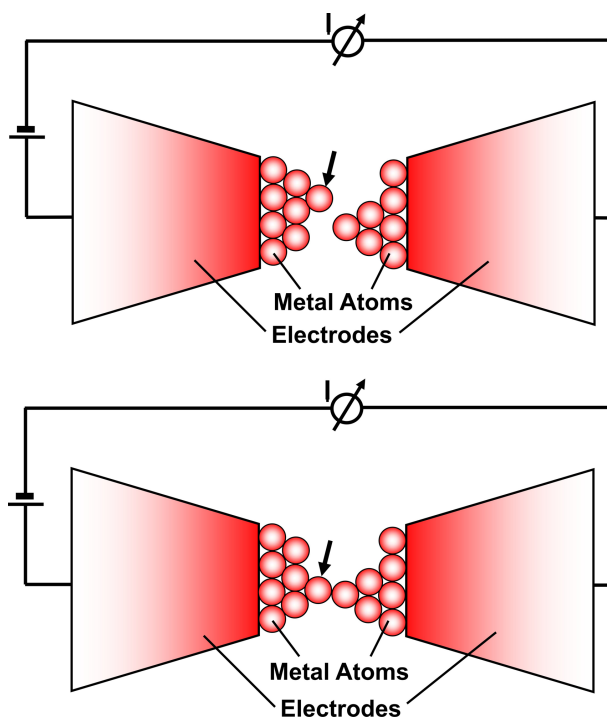


**Figure 2.** Schematic of the switching process: A metal atom (see arrow) is switched between a quantized conducting “on-state” (lower graph) and an insulating “off-state” (upper graph).

The potentials of the working electrodes with respect to the quasi-reference and counter electrodes are set by a computer-controlled bipotentiostat (see Fig. 3). All experiments are performed at room temperature, the electrolyte being kept in ambient air. For conductance measurements, an additional voltage in the millivolt range is applied between the two gold

electrodes. To fabricate the atomic transistor, silver is deposited on each of the two working electrodes, until finally two silver crystals meet, forming an atomic scale contact which is bridging the gap.

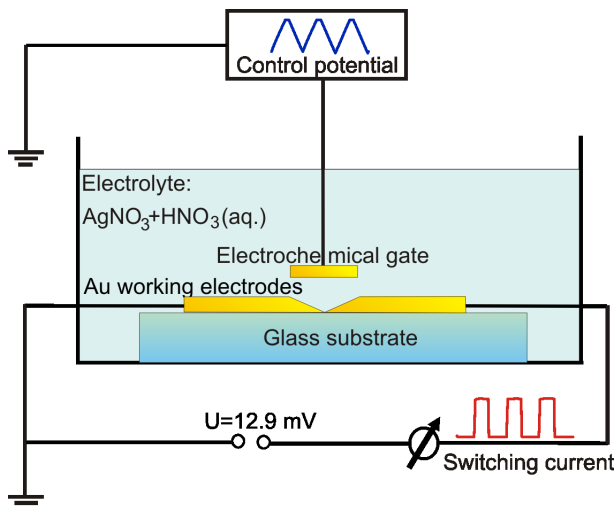
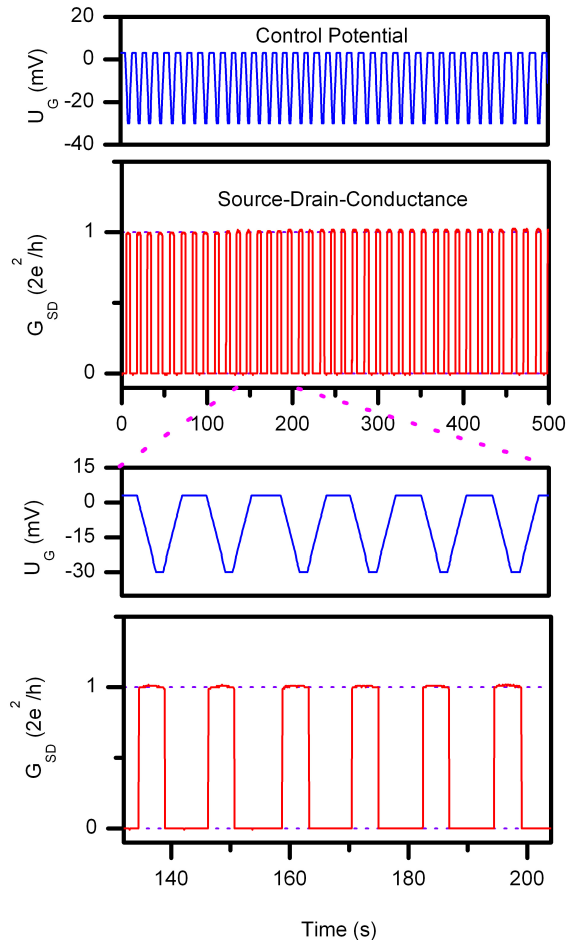


**Figure 3.** The experimental setup. Within a narrow gap between two gold electrodes on a glass substrate, a silver point contact is deposited electrochemically. By a procedure involving repeated computer-controlled electrochemical cycling, a bistable atomic-scale quantum conductance switch is fabricated.

While silver islands are deposited in the junction we monitor the conductance between the two electrodes. As soon as the conductance exceeds a preset “target” value, the deposition is stopped and the voltage is reversed to dissolve the junction again. After the conductance drops below a preset value, the deposition/dissolution cycle is repeated automatically by the computer-controlled setup. During the first cycles, the conductance at the end of the deposition step varies strongly from cycle to cycle [11]. After repeated cycling, an abrupt change is observed from this irregular variation to a bistable switching between zero and a finite, quantized conductance value at an integer multiple of  $G_0 (= 2e^2/h)$ .

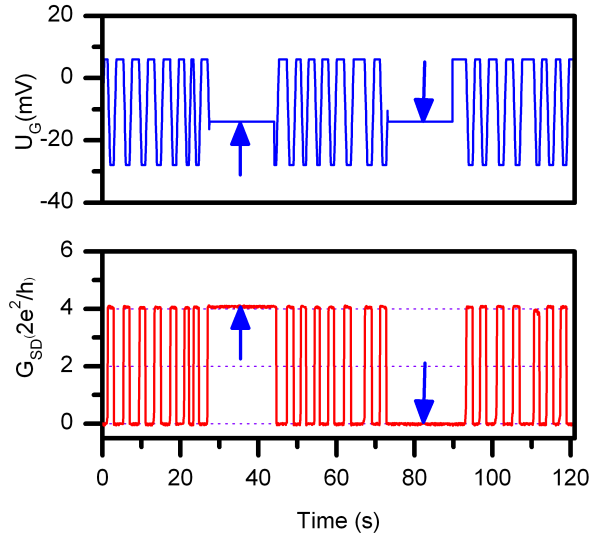
### ***Controlling the junction at the single-atom level***

Figure 4 shows a sequence of reproducible switching events between an insulation “off-state” and a quantized conducting “on-state” (at  $1 G_0$ ), where the quantum conductance (red curves) of the switch is controlled by the gate potential (blue curves), as commonly observed in transistors. As calculations have shown [10], for atomic-scale silver contacts a quantized conducting “on-state” of  $1 G_0$  corresponds to a *single-atom* contact.



**Figure 4.** Switching an electrical current by gate-controlled atomic movement: Experimental data of reproducible electrical switching with a single silver atom point contact between an “on-state” at  $1 G_0$  ( $1 G_0 = 2e^2/h$ ) and a non-conducting “off-state”. The source-drain conductance ( $G_{SD}$ ) of the atomic switch (red curves) is directly controlled by the gate potential ( $U_G$ ) (blue curves).

When we set the gate potential to an intermediate “hold” level between the “on” and the “off” potentials, the currently existing state of the atomic switch remains stable, and no further switching takes place. This is demonstrated in Figure 5 both for the “on-state” of the switch (left arrow) and for the “off-state” of the switch (right arrow). Thus, the switch can be reproducibly operated by the use of three values of the gate potential for “switching on”, “switching off” and “hold”. These results give clear evidence of a hysteresis when switching between the two quantized states of the switch. It can be explained by an energy barrier which has to be overcome when performing the structural changes within the contact when switching from the conducting to the non-conducting state of the switch and *vice versa*.



**Figure 5.** Demonstration of quantum conductance switching between a non-conducting “off-state” and a preselected quantized “on-state” at  $4 G_0$ . A conductance level can be kept stable, if  $U_G$  is kept at a “hold” level (see arrows) (cf. [1]).

The results indicate that switching occurs by a reversible rearrangement of the contacting group of atoms between two different stable configurations with a potential barrier between them. For silver the observed quantum conductance levels appear to coincide with *integer* multiples of the conductance quantum [1, 10].

The observed integer conductance levels of the switch are determined by the available bistable junction conformations, similar to the observation of preferential atomic configurations in metallic clusters corresponding to “magic numbers” [12]. By snapping into ‘magic’ bistable conformations, such energetically preferred junction configurations are mechanically and thermally stable at room temperature, and they are reproducibly retained even during long sequences of switching cycles.

### ***Multilevel Switching***

Reproducible switching in the above cases was always performed by opening and closing a quantum point contact, i.e. by switching between a quantized conducting state and a non-conducting state. However, it was not clear if this kind of gate-electrode controlled switching is also possible between two different conducting states of one and the same contact. Such kind of switching would involve two different stable contact configurations on the atomic scale, between which reversible switching would occur even without ever breaking the contact.

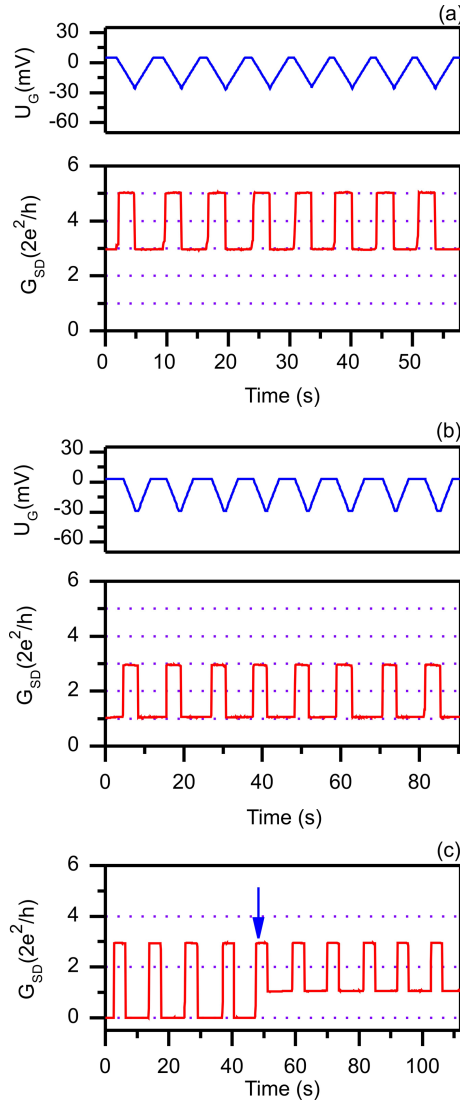


**Figure 6.** (a) and (b): Experimental demonstration of the operation of an *interlevel* transistor based on an atomic-scale silver quantum point contact. A controlled change of the electrochemical gate potential  $U_G$  leads to controlled switching of the conductance of the quantum point contact  $G_{SD}$  between *two different* quantized conducting states each of which is different from zero. The upper diagram gives the control potential (blue curve) applied to a “gate” electrode while the lower shows the corresponding conductance switching of the point contact (red curve). The two states between which the switching occurs in (a) exhibit conductance levels of  $3 G_0$  ( $G_0 = 2e^2/h$ ) and  $5 G_0$ , respectively. (b) Example of another *interlevel* quantum transistor switching between the conductance levels of  $1 G_0$  and  $3 G_0$ . (c) Experimental demonstration of a multi-level atomic-scale transistor switching between an “off-state” and two different “on-states” (cf. [13]).

Such multi-level logics and storage devices on the atomic scale would be of great interest as they allow a more efficient data storage and processing with a smaller number of logical gates. By developing a modified procedure of fabrication, a multi-level atomic quantum transistor was obtained, allowing the gate-controlled switching between *different* conducting states.

Instead of setting the lower threshold where the dissolution process is stopped by the computer, to a value near  $0 G_0$ , the lower threshold was set at a value above the desired quantized conductance of the lower of the two “on-state” levels [13].

Figure 6 demonstrates the operation of such a two-level transistor: A controlled change of the gate potential  $U_G$  leads to a controlled switching of the conductance of the quantum point contact between two *different* quantized conducting states (for details see caption of Fig. 6). Sharp transitions are observed between the two levels. No intermediate steps or staircase-like structures in conductance are observed in the diagram. The transitions are instantaneous within the time resolution of the diagram of Figure 6 (50 ms).

## COMPUTER SIMULATIONS OF THE SWITCHING PROCESS

Reproducible switching between quantum conductance levels over many cycles cannot be explained by conventional atom-by-atom deposition but requires a collective switching mechanism. Our calculations have shown that only well-ordered junction geometries result in integer multiples of the conductance quantum [10]. Neither partial dissolution of the junction nor its controlled rupture yields the necessary atomic-scale memory effect. A more detailed model of the structural [15, 16] and conductance [3, 17] properties of such junctions is therefore required.

We begin with the unbiased deposition of silver ions (Fig. 7a), which evolve under the influence of the electrostatic potential of the electrodes [18]. Starting from two distant parallel Ag(111) layers, we evolve each ion in the long-range electrostatic potential generated from the present electrode conformation and a short-range Gupta potential for silver [19]. In the simulations, we deposit one atom at a time using a kinetic Monte Carlo method [18] starting at a random position inside the junction. We deposit up to 800 atoms in the junction until a predefined number of non-overlapping pathways connect the left and right electrode. As a non-overlapping pathway, we define a unique set of touching atoms that extend from one electrode to the other, which permits us to identify the minima cross-section of the junction.

---



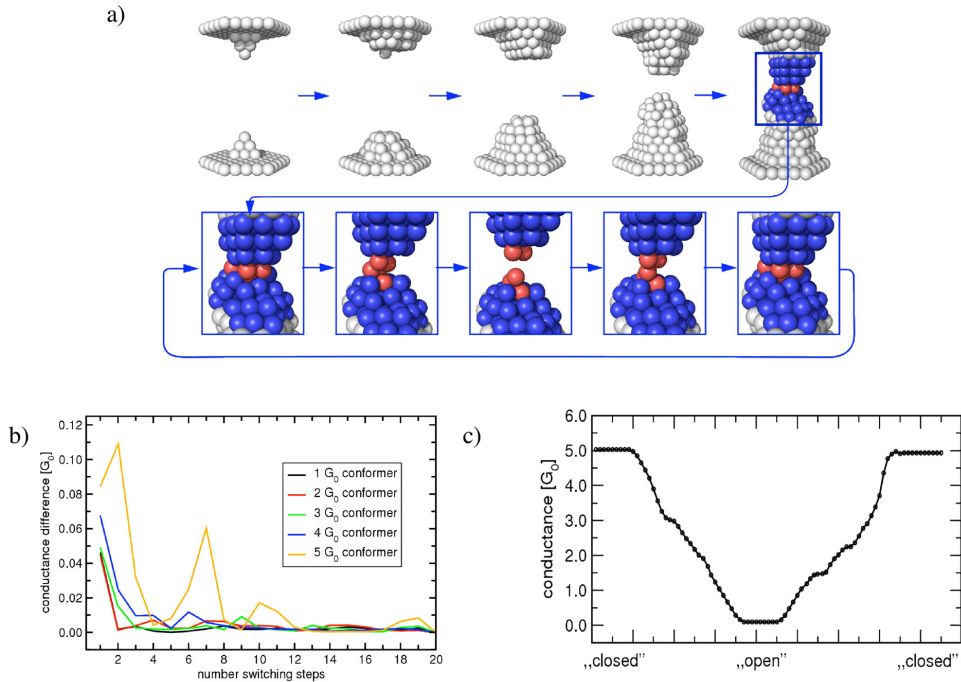


**Figure 7.** Simulation of atomic point contact growth and switching process. **(a)** Snapshots of the deposition simulation. Upper row: The growth process starts with two disconnected Ag(111) layers and stops, when a non-overlapping pathway with a predefined number of silver atoms connects the electrodes. Lower row: Simulation of the switching process reveals a bistable tip reconstruction process as the mechanism underlying the reproducible switching of the conductance. During the simulation, we kept the silver atoms marked in gray at their positions at the end of the deposition and permitted the central cluster of atoms to evolve (blue and red atoms) under the influence of the electrochemically induced pressure. The central silver atoms (red) define the minimal cross-section. These atoms return with sub-Ångström precision to their original positions at the end of the switching cycle. **(b)** Difference in the computed conductance between subsequent “on” conformations as a function of the switching cycle for selected junctions of 1  $G_0$ , 2  $G_0$ , 3  $G_0$ , 4  $G_0$ , and 5  $G_0$ , respectively. Junctions switch reproducibly for over 20 cycles between increasingly stable “on” and “off” conformations (training effect). **(c)** Variation of the computed conductance of a 5  $G_0$  switch during one “open-close” process. In agreement with the experimental observations, we find asymmetric plateaus in the conductance curve, if the switch is opened or closed. This can be traced back to the existence of several low-energy pathways connecting the open and closed state (cf. [1]).

Next, we simulate the switching process: The change in the electrochemical potential induces a change in the interface tension of the liquid-metal interface, making possible a deformation of the junction geometry parallel to the junction axis. It is well-known that changes in the electrochemical potential modulate the interfacial tension of the whole electrode [20–22] which results in a mechanical strain on the junction. We simulate the

opening/closing cycle of a junction by evolving the atoms of a “central” cluster under the influence of the electrochemical pressure. We assume that only the atoms in this region move in the switching process, while most of the bulk material remains unchanged. The central cluster comprises the atoms of the minimal cross-section connecting the two electrodes and all atoms within a radius of 9.0 Å around this central bottleneck. While the electrodes gradually move apart/closer together, all atoms of the central cluster relax in simulated annealing simulations generating a quasi-adiabatic path between the open and the closed conformation.

Not surprisingly, the junction rips apart at some finite displacement from the equilibrium, an effect also seen in break-junction experiments. For most junctions, this process is accompanied by a surface reorganization on at least one, but often both, tips of the electrode(s). When we reverse the process, some junctions snap into the original atomistic conformation with subatomic precision. Figure 8 shows the simulated contact geometries (b) and the related minimum cross sections (c) for 1...5  $G_0$  together with the corresponding experimentally determined switching curves (a). At the end of the switching simulation, we compare the final and the starting geometry. If after the first switching cycle the junction has returned to the same geometry, we consider the junction “switchable” and perform further switching cycle simulations to test stability. Otherwise, we discard the junction completely and start from scratch.

We have performed 15280 full deposition simulations generating  $N_{\text{conf}} = 17, 8, 3, 17,$  and 6 junctions with  $p = 1, \dots, 5$  conductance quanta, respectively. Most deposition simulations fail to generate a switchable junction because the “acceptance criterion” for “switchability” was very strict. We note that the same holds true for most control simulations starting from the “perfect” conformations of [10], indicating that simple rupture of even nearly ideal junctions cannot be the basis of the switching mechanism.

We then compute the zero-bias conductance [23 – 25] of the entire junction using a material-specific, single particle Hamiltonian and realistic electrode Green’s functions [26]. We use a recursive Green’s function method [27, 28] which maps the problem of computing the full device Green’s function to the calculation of “principal layer” Green’s functions, which drastically reduces the computational effort but maintains the accuracy. The electronic structure is described using an extended Hückel model including s-, p-, and d-orbitals for each silver atom (7200 orbitals per junction [29] in the standard minimal basis set of non-orthogonal Slater type orbitals. We take the influence of the leads into account, by assuming a semi-infinite fcc lattice for the left and the right reservoir. We compute the material-specific surface Green’s functions by applying a decimation technique that exploits the translational symmetry of the semi-infinite contacts [30]. We find that the retained junction conformations (typically comprising 500 – 800 atoms) have a preselected integer multiple ( $n$ ) of  $G_0$  in close agreement with the experiment. The direct comparison of our atomistic, quantum conductance calculations, using the unaltered conformations from the deposition/

---

switching simulations, with the experimental conductance measurements offers a strong validation of the geometries generated in our deposition protocol. The observed agreement between computed and measured conductance is impressive, because the conductance of metallic wires is well-known to be strongly dependent on the geometry.

We have repeated this process up to 20 times for each junction (Fig. 7b) and observe a “training effect”, in which the junction geometries become increasingly stable, alternating between two bistable conformations. When re-computing the zero-bias conductance at the end of switching cycle, we find the same value as for the original junction (to within  $\sim 0.05 G_0$ ). Because these observations result from completely unbiased simulations of junction deposition and switching, they explain the observed reversible switching on the basis of the generation of bistable contact geometries during the deposition cycle. If we consider the tip-atoms at each side of the electrodes in the open junction, the equilibrium geometry of both clusters depends on their environment. In the open junction, this environment is defined by the remaining electrode atoms on one side, while in the closed junction, the tip-cluster of the other electrode is also present. Our simulations demonstrate the existence of two stable geometries for each cluster in both environmental conditions, respectively. Reversible switching over many cycles is thus explained by reversible tip reorganization under the influence of the gate potential, similar to induced surface reorganization [31 – 33]. While the overall structure differs between junctions with the same conductance quantum from one realization to the next (see Fig. 8b for representative examples), the minimal cross-section that determines the conductance is largely conserved (Fig. 8c). When comparing the opening process and the closing process of the junction, we observe asymmetric conductance curves (see Fig. 7c), in agreement with experiment, resulting from irreversible low-energy pathways between the open and the closed conformations.

These data rationalize the bistable reconfiguration of the electrode tips as the underlying mechanism of the formation of nanoscale junctions with predefined levels of quantum conductance. These levels are determined by the available bistable junction conformations, similar to magic numbers for metal clusters [33] that are most likely material-specific. For silver, the observed quantum conductance levels appear to coincide with integer multiples of the conductance quantum. When we form a junction by halting the deposition process at a non-integer multiple of  $G_0$  (both experimentally and in simulation), subsequent switching cycles either converge to an integer conductance at a nearby level or destroy the junction. By snapping into “magic” bistable conformations, junctions are mechanically and thermally stable at room temperature for long sequences of switching cycles. This process is assisted by the electrochemical environment but not intrinsically electrochemical: The reproducible switching of large junctions by coordinated dissolution/regrowth of the junction is very unlikely.

---

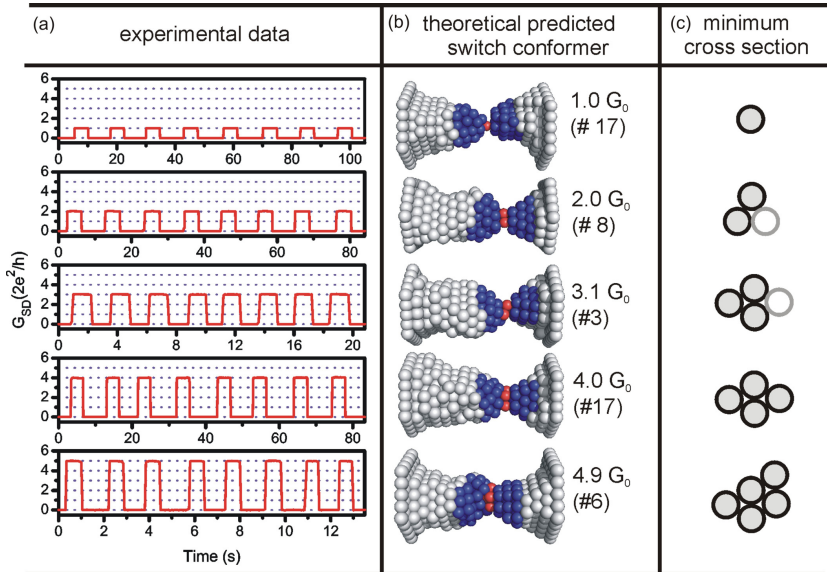


**Figure 8.** Relation between the structures of atomic point contacts and their conductance. **(a)** Quantum conductance switching between a non-conducting “off-state” and a preselected quantized “on-state” at 1  $G_0$ , 2  $G_0$ , 3  $G_0$ , 4  $G_0$ , and 5  $G_0$ , respectively (note individual time axis). **(b)** Representative conformations of simulated junctions, computed zero-bias conduction, and number of junctions with the specified conductance. **(c)** Representative minimal cross-sections for each conductance level. The minimal cross-sections are characteristic for each group of the switch conformers and determine their quantized conductance (cf. [1]).

## CONCLUSIONS AND PERSPECTIVES

The development of the single-atom transistor represents a first demonstration of the functionality of a transistor on the atomic scale. This is of great interest, as there were many previous demonstrations of passive devices such as atomic-scale and molecular resistors. However, there was a lack of an actively switching device such as a transistor on the atomic scale. The atomic transistor as an actively controllable device, which reproducibly operates at room temperature, is filling this gap.

The switching process is explained by a reproducible rearrangement of individual atoms between two well-defined geometries. Computer simulations are in excellent agreement with the experimental results and show the self-stabilization of the switching process.

Atomic transistors represent a new class of devices which show remarkable properties:

- They allow the switching of an electrical current by the *geometrical relocation of individual atoms* rather than by locally changing electronic properties as done in conventional transistors.
- They represent *quantum switches*, the levels between which the switching occurs being given by fundamental laws of quantum mechanics.
- They are a first demonstration of an *all-metal transistor* without the use of any semiconductor, the lack of a band gap allowing operation at very low voltages.

Such devices provide a number of advantages: They possess extremely nonlinear current-voltage characteristics, desirable in many applications, and they can be manufactured using conventional, abundant, inexpensive and non-toxic materials. At the same time, the devices open perspectives for electronic switching at ultrafast frequencies: although the switching time in our current investigations is limited by the response time of the electrodes (3–5 microseconds), the intrinsic operation time is expected to be limited by the atomic-scale rearrangement within the junction (picoseconds), opening perspectives for ultrahigh frequency operation. Because the switching process is achieved with very small gate potentials in the millivolt range, the power consumption of such devices is by orders of magnitude lower than that of conventional semiconductor-based electronics.

Although the development of the single-atom transistor just marks the beginning of actively controlled electronics on the atomic scale, it opens fascinating perspectives for quantum electronics and logics based on individual atoms. The development of a first, simple integrated circuit [1, 14] and a multilevel quantum transistor [13] are first encouraging steps in this direction.

### ACKNOWLEDGMENT

This work was supported by the Deutsche Forschungsgemeinschaft within the DFG Centre for Functional Nanostructures and by the Baden-Württemberg Foundation within the Network of Excellence on Functional Nanostructures, Baden-Württemberg. Part of the experimental section were reproduced with permission of *Europhysics News* (2010) [34], Figure 6 was reproduced with permission from *Advanced Materials* (Copyright 2010, Wiley-VCH) [13], Figures 7 and 8 with permission from *Nano Lett.* (ACS, Copyright 2010) [1].

---

**REFERENCES**

- [1] Xie, F.-Q., Maul, R., Augenstein, A., Obermair, Ch., Starikov, E.B., Schön, G., Schimmel, Th., Wenzel, W. (2008) *Nano Lett.* **8**:4493.  
doi: 10.1021/nl802438c.
  - [2] Agraít, N., Yeyati, A.L., van Ruitenbeek, J.M. (2003) *Phys. Rep.* **377**:81.  
doi: 10.1016/S0370-1573(02)00633-6.
  - [3] Scheer, E., Agraít, N., Cuevas, N.J., Levy Yeyati, A., Ludoph, B., Martin-Rodero, A., Rubio Bollinger, G., van Ruitenbeek, J.M., Urbina, C. (1998) *Nature* **394**:154.  
doi: 10.1038/28112.
  - [4] Mares, A.I., van Ruitenbeek, J.M. (2005) *Phys. Rev. B* **72**:205402.  
doi: 10.1103/PhysRevB.72.205402.
  - [5] Li, C. Z., Bogozí, A., Huang, W., Tao, N.J. (1999) *Nanotechnology* **10**:221.  
doi: 10.1088/0957-4484/10/2/320.
  - [6] Xie, F.-Q., Nittler, L., Obermair, Ch., Schimmel, Th. (2004) *Phys. Rev. Lett.* **93**:128303.  
doi: 10.1103/PhysRevLett.93.128303.
  - [7] Xie, F.-Q., Obermair, Ch., Schimmel, Th. (2004) *Solid State Communications* **132**:437.  
doi: 10.1016/j.ssc.2004.08.024.
  - [8] Smith, D.P.E. (1995) *Science* **269**:371.  
doi:10.1126/science.269.5222.371.
  - [9] Terabe, K., Hasegawa, T., Nakayama, T., Aono, M. (2005) *Nature* **433**:47.  
doi: 10.1038/nature03190.
  - [10] Xie, F.-Q., Maul, R., Brendelberger, S., Obermair, Ch., Starikow, E.B., Wenzel, W., Schön, G., Schimmel, Th. (2008) *Appl. Phys. Lett.* **93**:043103.  
doi: 10.1063/1.2955521.
  - [11] Xie, F.-Q., Obermair, Ch., Schimmel, Th. (2006) In: R. Gross *et al.* (eds.), *Nanoscale Devices - Fundamentals and Applications*. Springer, p153.
  - [12] Huda M.N., Ray, A.K., (2003) *Phys. Rev. A* **67**:013201.  
doi: 10.1103/PhysRevA.67.013201.
  - [13] Xie, F.-Q., Maul, R., Obermair, Ch., Schön, G., Wenzel, W., Schimmel, Th. (2010) *Advanced Materials* **22**:2033.  
doi: 10.1002/adma.200902953.
  - [14] Schimmel, Th., Xie, F.-Q., Obermair, Ch. Patent pending, US 2009195300.
-

- [15] Pauly, F., Dreher, M., Viljas, J.K., Häfner, M., Cuevas, J.C., Nielaba, P. (2006) *Phys. Rev. B* **74**:235106.  
doi: 10.1103/PhysRevB.74.235106.
- [16] Yanson, I.K., Shklyarevskii, O.I., Csonka, S., van Kempen, H., Speller, S., Yanson, A.I., van Ruitenbeek, J.M. (2005) *Phys. Rev. Lett.* **95**:256806.  
doi: 10.1103/PhysRevLett.95.256806.
- [17] Yanson, A.I., Yanson, I.K., van Ruitenbeek, J.M. (2001) *Phys. Rev. Lett.* **87**:216805.  
doi: 10.1103/PhysRevLett.87.216805.
- [18] Kwiatkowski, J.J., Nelson, J., Li, H., Bredas, J.L., Wenzel, W., Lennartz, C. (2008) *Phys. Chem. Chem. Phys.* **10**:1852.  
doi: 10.1039/b719592c.
- [19] Shao, X., Liu, X., Cai, W.J., (2005) *J. Chem. Theory Comput.* **1**:762.  
doi: 10.1021/ct049865j.
- [20] Weissmuller, J., Viswanath, R.N., Kramer, D., Zimmer, P., Wurschum, R., Gleiter, H. (2003) *Science* **300**:312.  
doi: 10.1126/science.1081024.
- [21] Weigend, F., Evers, F., Weissmüller, J. (2006) *Small* **2**:1497.  
doi: 10.1002/sml.200600232.
- [22] Inglesfield, J.E. (1985) *Prog. Surf. Sci.* **20**:105.  
doi: 10.1016/0079-6816(85)90007-3.
- [23] Xue, Y., Datta, S., Ratner, M. (2002) *Chem. Phys.* **281**:151.  
doi: 10.1016/S0301-0104(02)00446-9.
- [24] Heurich, J., Cuevas, J.C., Wenzel, W., Schön, G. (2002) *Phys. Rev. Lett.* **88**:256803.  
doi: 10.1103/PhysRevLett.88.256803.
- [25] van Zalinge, H., Bates, A., Schiffrin, D.J., Starikov, E.B., Wenzel, W., Nichols, R.J. (2006) *Angew. Chem.* **45**:5499.  
doi: 10.1002/anie.200601263.
- [26] Jacob, T. (2007) *Electrochim. Acta* **52**:2229.  
doi: 10.1016/j.electacta.2006.03.114.
- [27] Vergés, J.A. (1999) *Comput. Phys. Commun.* **118**:71.  
doi: 10.1016/S0010-4655(99)00206-4.
- [28] Maul, R., Wenzel, W. (2009) *Phys. Rev. B* **80**:045424.  
doi: 10.1103/PhysRevB.80.045424.
-

- [29] Starikov, E.B., Tanaka, S., Kurita, N., Sengoku, Y., Natsume, T., Wenzel, W. (2005) *Eur. Phys. J. E* **18**:437.  
doi: 10.1140/epje/e2005-00047-4.
- [30] Damle, P., Ghosh, A.W., Datta, S. (2002) *Chem. Phys.* **281**:171.  
doi: 10.1016/S0301-0104(02)00496-2.
- [31] Ohiso, A., Sugimoto, Y., Abe, M., Morita, S. (2007) *Jpn. J. Appl. Phys.* **46**:5582.  
doi: 10.1143/JJAP.46.5582.
- [32] Ternes, M., Lutz, C.P., Hirjibehedin, C.F., Giessibl, F.J., Heinrich, A.J. (2008) *Science* **319**:1066.  
doi: 10.1126/science.1150288.
- [33] Huda, M.N., Ray, A.K. (2003) *Phys. Rev. A* **67**:013201.  
doi: 10.1103/PhysRevA.67.013201.
- [34] Obermair, Ch., Xie, F.-Q., Schimmel, Th. (2010) *Europhysics News* **41**:25.  
doi: 10.1051/ePN/2010403.
-